To the Graduate Council:

I am submitting herewith a thesis written by Yixiang Frank Zhang entitled "Detecting Fabric Defects By Image Analysis." I have examined the final copy of this thesis for form and content and recommend that it be accepted in partial fulfillment of the requirements for the degree of Master of Science, with a major in Computer Science.

M. Thomason, Major Professor

We have read this thesis
and recommend its acceptance:

Accepted for the Council:

Associate Vice Chancellor
and Dean of The Graduate School

DETECTING FABRIC DEFECTS BY IMAGE ANALYSIS

A Thesis
Presented for the
Master of Science
Degree
The University of Tennessee, Knoxville

Yixiang Frank Zhang
December, 1993

Copyright © Yixiang Frank Zhang, 1993
All rights reserved

ACKNOWLEDGEMENTS

I would like to express my sincerest gratitude to my major advisor, Dr. Michael Thomason, for his unusual patience, understanding, continued support throughout all phases of this thesis.

I am very thankful to Dr. Jens Gregor, for his precious technical advice. I also want to acknowledge Dr. Randall R. Bresee for his encouragement and suggestions in the research. My deep appreciation goes to Dr. X. C. Huang for his friendship and invaluable suggestions.

During my graduate study, I received encouragement and help from Dr. David Straight, Dr. David Mutchler, Dr. Michael Vose and Ms. Wallace Mayo. My special appreciation also goes to my caring and supportive friends: Cindy Wang, Mr. and Mrs. Wei Wang, and Mr. and Mrs. Robert Pederson.

Most of all, I wish to express my deepest gratitude to my parents, my brother and sister-in-law, who have been giving me unconditional love and support all the time.

ABSTRACT

A method of detecting defects in solid-shade, unpatterned woven fabrics is described. Two types of defects are studied: knots and slubs. The proposed automatic inspection system consists of a unix workstation, video camera, frame grabber and illumination device. Fabric samples are illuminated with transmitted light. A digitized picture from the video camera is stored in the memory of the computer. The computer calculates features from the picture and classifies samples as defective or defect-free. The locations of defects are also indicated. Autocorrelation function is used to determine the size of the repeat unit in the picture. Two approaches to detecting defects, gray level statistics and morphological operations, are presented. Fabric products from a local textile mill are examples of objects for inspection.

TABLE OF CONTENTS

CHAPTER			PAGE
1.	**Introduction**		**1**
2.	**Fabric Defects**		**3**
3.	**Image Processing**		**5**
	3.1	Histogram Equalization	5
	3.2	Thresholding	12
	3.3	Morphology	16
		3.3.1 Erosion and Dilation	16
		3.3.2 Opening and Closing	18
	3.4	Autocorrelation	19
4.	**Instrumentation and Experiment Design**		**23**
	4.1	Instrumentation	23
		4.1.1 Hardware	23
		4.1.2 Software	24
	4.2	Experimental Material	24
		4.2.1 Material	24
		4.2.2 Detecting Fabric Defects	24
5.	**Results and Discussion**		**28**
	5.1	Gray level statistical approach	28
		5.1.1 Repeat unit size and selection of test window size	28
		5.1.2 Lower limit of the average gray level in the test window	29
		5.1.3 The connectivity between defective windows and defects classification	33
	5.2	Morphological operation approach	40
		5.2.1 The selection of kernel size	40
		5.2.2 Detection and classification of defects	44
6.	**Summary and Recommendations**		**51**
	6.1	Summary	51
	6.2	Recommendations	52

BIBLIOGRAPHY 53
Reference 54

VITA 58

LIST OF FIGURES

FIGURE		PAGE
2.1	An example of a fabric with a knot.	3
2.2	An example of a fabric with a slub.	4
3.1	An example of bright image	6
3.2	An example of dark image	6
3.3	Histogram of the bright image	7
3.4	Histogram of the dark image	7
3.5	Bright image subjected to histogram equalization	8
3.6	Dark image subjected to histogram equalization	8
3.7	Histogram of the bright image after histogram equalization	9
3.8	Histogram of the dark image after histogram equalization	9
3.9	An image of a fabric with a knot and its histogram	10
3.10	The image after histogram equalization and its histogram	11
3.11	Gray level distribution of pixels in defective areas	13
3.12	Histogram equalized image	14
3.13	Gray level histogram of equalized image	14
3.14	Result of histogram equalization and segmentation with T=129	15
3.15	A equalized and thresholded image	17
3.16	Structuring element of size of 6X6	17
3.17	Image subjected to erosion by structuring element of size 6X6	17
3.18	Image subjected to opening by structuring element of size 6X6	18
3.19	An example of a repeat pattern	20
3.20	An example of fabric image	21
3.21	Autocorrelation function $C_{x,0}$ of sample image	22
3.22	Autocorrelation function $C_{0,y}$ of sample image	22
4.1	Gray level statistical approach	25
4.2	Illustration of overlap windows	26
4.3	Morphological operation approach	27
5.1	A simple image of a fabric with a slub	31
5.2	Test result of using factor z of 3.60	31
5.3	Test result of using factor z of 3.54	32
5.4	Test result of using factor z of 3.10	32
5.5	An example of a fabric with a slub	34
5.6	Average gray level in each window	34
5.7	Gray level statistical test result	34

5.8 An example of a fabric with a knot 36
5.9 Average gray level in each window 36
5.10 Gray level statistical test result 36
5.11 An example of a fabric with a slub 37
5.12 Average gray level in each window 37
5.13 Gray level statistical test result 37
5.14 An example of a fabric with a knot 38
5.15 Average gray level in each window 38
5.16 Gray level statistical test result 38
5.17 Autocorrelation function $C_{x,0}$ of twill weave sample G 41
5.18 Autocorrelation function $C_{0,y}$ of twill weave sample G 41
5.19 An image of a fabric with a slub 42
5.20 Image subjected to opening by structuring element of 8X3 . . 42
5.21 Image subjected to opening by structuring element of 7X3 . . 43
5.22 Image subjected to opening by structuring element of 8X2 . . 43
5.23 An example of a fabric with a slub 46
5.24 Image subjected to erosion by structuring element of size 8X4 46
5.25 Image subjected to opening by structuring element of size 8X4 46
5.26 An example of a fabric with a knot 47
5.27 Image subjected to erosion by structuring element of size 8X4 47
5.28 Image subjected to opening by structuring element of size 8X4 47
5.29 An example of a fabric with a slub 48
5.30 Image subjected to erosion by structuring element of size 6X6 48
5.31 Image subjected to opening by structuring element of size 6X6 48
5.32 An example of a fabric with a knot 49
5.33 Image subjected to erosion by structuring element of size 6X6 49
5.34 Image subjected to opening by structuring element of size 6X6 49

LIST OF TABLES

TABLE		PAGE
3.1	The comparison of distribution of pixels in defective areas with the normal distribution	13
5.1	The standard deviations of gray level average in windows of different size.	29
5.2	Test results using different lower limits.	30
5.3	The repeat unit size and statistics of samples	35
5.4	The gray level statistical test results	39
5.5	The repeat unit size and kernel size of samples	44
5.6	The morphological operation test results	50

CHAPTER 1

Introduction

Quality control plays an important role in textile manufacturing. The last process of the weaving industry and the first process of the apparel manufacturing is fabric inspection. At present, fabric defect detection is carried out by human operators and is therefore a subjective process. Human inspection is expensive, tedious and time-consuming and the quality varies from person to person.

Automatic inspection is an alternative to the human inspector for several practical reasons: (1) freeing humans from the routine; (2) saving labor cost; (3) performing consistent inspection in unfavorable environments; (4) speeding inspection process; (5) analyzing statistics on test information and keeping records for management decision [5].

Advances in technology have resulted in better, cheaper image-analysis equipment. These advances, combined with those of image processing and pattern recognition technologies, make it possible to inspect fabric products automatically in ordinary factories.

Automated visual inspection systems have been developed and utilized in a number of industries. The electronic industry uses computerized visual inspection systems to control the quality of printed circuit patterns [18] [24] and microcircuit photomasks [31] and to inspect electronic assemblies [20]. Automobile [32], lumber [6], and metal processing [7] [21] industries also use automated visual inspection system for monitoring and testing.

Recently, computer techniques have expanded considerably in textile manufacturing and testing. Using computer image processing, blend irregularity in yarns is evaluated [30], pile-fiber distribution in sliver-knitted fabric [14] and cuticular scales [22] are measured, and warp stripness [15] and fabric appearance [4] are studied. Image processing techniques are also used in the development of cotton trashmeter [27] [28]. A number of research papers have been published on carpet texture measurement using image analysis [26] [33] [34] [35] [36]. Researchers in America, Germany and Japan introduced image analysis techniques into woven and nonwoven textile fabric monitoring, testing, and defects detecting [1] [16] [17] [19] [10] [23] [25].

Fabrics can be classified into three categories: 1) solid-shade, unpatterned textiles, 2) large-patterned textiles and 3) small-patterned textiles [1]. This thesis presents a method which permits certain defects on solid-shade, unpatterned textile to be detected.

The automatic inspection procedure has two stages: training and detection. In the training stage, prototypes of fabric construction are studied and models for these fabric constructions are developed. In the detection stage, the fabrics being inspected are compared with the construction models and deviations are categorized as defects. The locations of defects are also indicated and recorded for repairs and grading.

CHAPTER 2

Fabric Defects

Woven fabric consists of two systems of yarn which interlace at right angles to each other [8]. The lengthwise threads are called warp; individually they are known as ends. The crosswise threads are called filling or weft; individually, they are called picks. Weaving is done on a loom which interlaces the warp and filling threads according to a pre-arranged design. There are three basic weaves: plain weave, twill weave and satin weave. Because of mechanical problems on looms and defects on the warp and filling, some parts of fabric may have deviant appearance from the pre-arranged design. These fabric parts are called fabric defects.

The defects which are likely to appear on the fabric were determined by questioning experienced inspectors. They are knots and slubs.

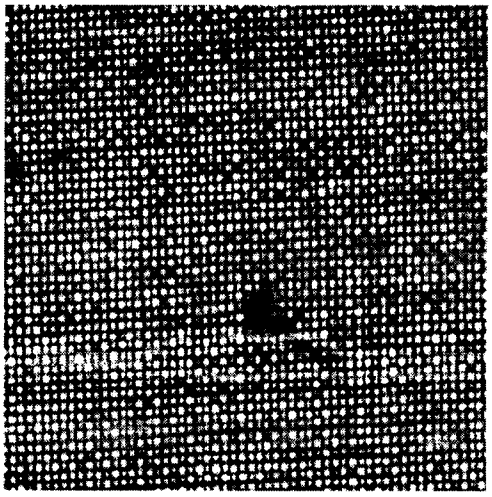


Figure 2.1: An example of a fabric with a knot.

As illustrated in Figure 2.1, a knot is an abruptly thickened round spot on the fabric surface. It is usually caused by knots on yarn and entanglement of fillings and warps. The minimum size of a knot depends on the coarseness of the yarn. If four or more yarns in the same yarn system are involved in the

entanglement and form a visible round shape spot on the surface of fabric, it will be categorized as knot. Figure 2.2 shows an example of a slub on fabric. A slub is an abruptly thickened line in horizontal or vertical direction on the fabric surface. It is usually caused by double pick, double end, and coarse pick [2] [3].

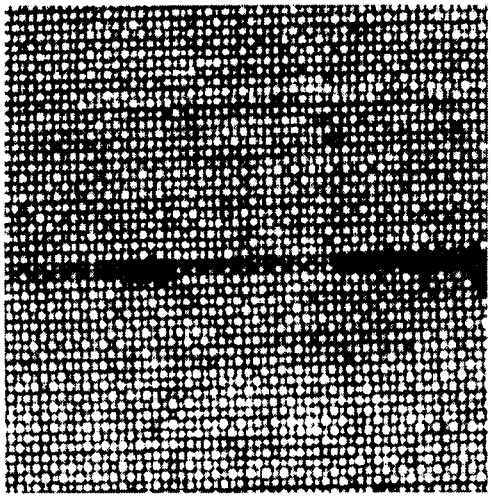


Figure 2.2: An example of a fabric with a slub.

CHAPTER 3

Image Processing

3.1 Histogram Equalization

Histogram equalization is a process in which gray level values are reassigned to produce a flattened histogram with a more uniform gray level distribution. The definition and algorithm of histogram equalization can be found in numerous publications [11] [12] [13].

Two images of same kind of fabric are shown in Figure 3.1 and 3.2. They were taken under the same image-acquisition conditions. By observing these two images and studying their gray level histograms shown in Figure 3.3 and 3.4, we see that their brightness and contrast are different. It is caused mainly by the variation of fabric thickness and noise.

In order to remove variation due to image capture conditions and make images of same kind of fabric more comparable to each other, histogram equalization using a standard algorithm [13] is employed.

Figures 3.5 and 3.6 show the result of histogram equalization. Figure 3.7 and 3.8 show the histograms of the equalized images. The gray levels of these two images that have been subjected to histogram equalization are spread out and reach dark and white. Histogram equalization increases the dynamic range of gray levels and produces an increase in image contrast. These two histogram equalized images become more comparable to each other since they have similar contrast and brightness.

Figures 3.9 and 3.10 show another example of histogram equalization. Figures 3.9 shows a dark fabric image and its histogram. The contrast of the image is so low that few texture details are revealed in the image. Figures 3.9 shows the image subjected to histogram equalization and its histogram. The contrast and brightness of the image are increased and details in the image are enhanced.

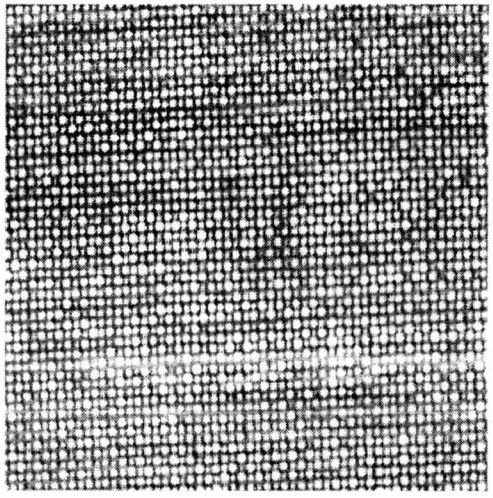


Figure 3.1: An example of bright image

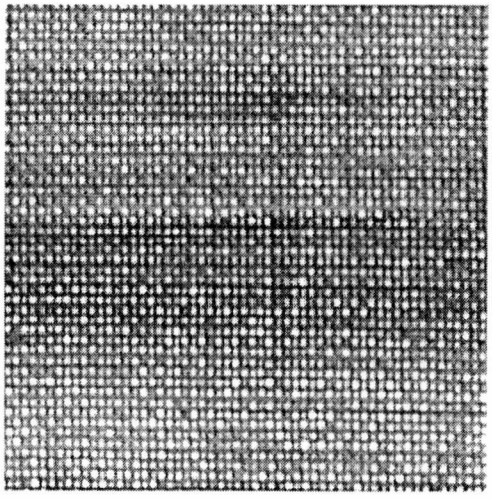


Figure 3.2: An example of dark image

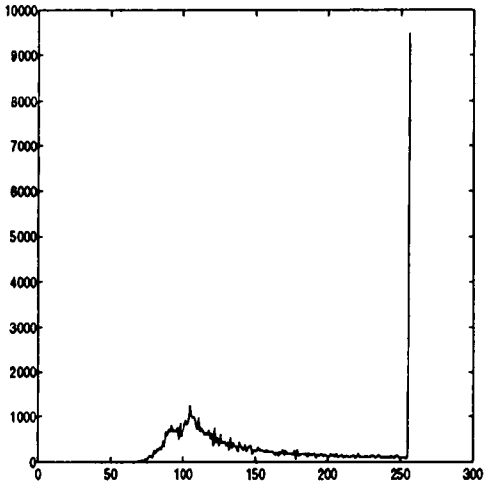


Figure 3.3: Histogram of the bright image

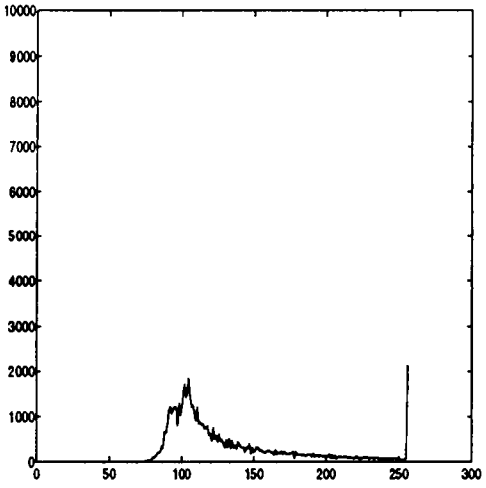


Figure 3.4: Histogram of the dark image

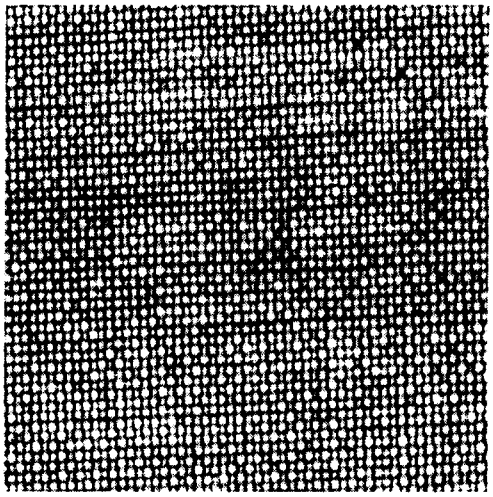


Figure 3.5: Bright image subjected to histogram equalization

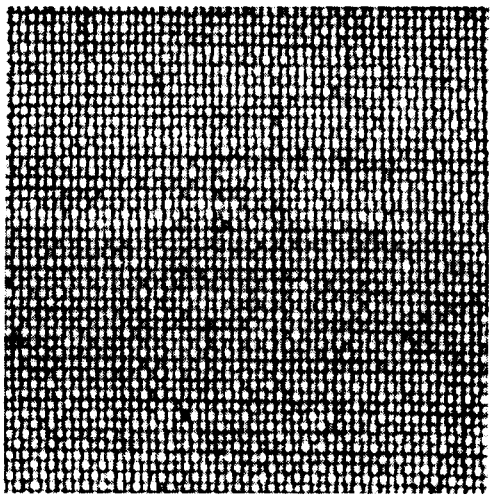


Figure 3.6: Dark image subjected to histogram equalization

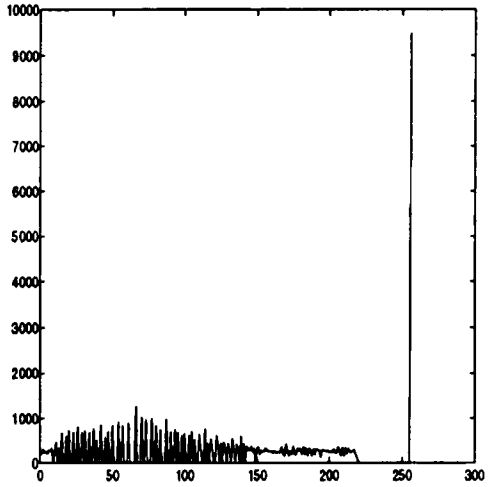


Figure 3.7: Histogram of the bright image after histogram equalization

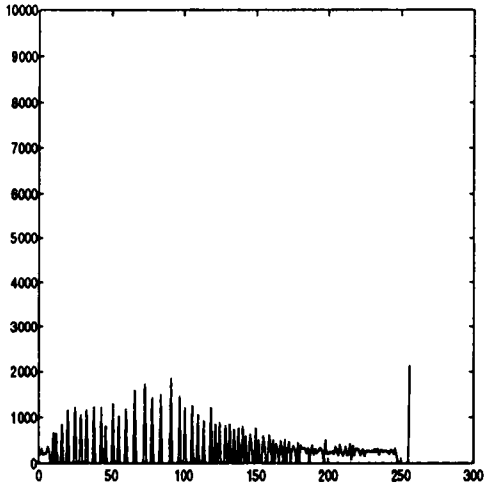


Figure 3.8: Histogram of the dark image after histogram equalization

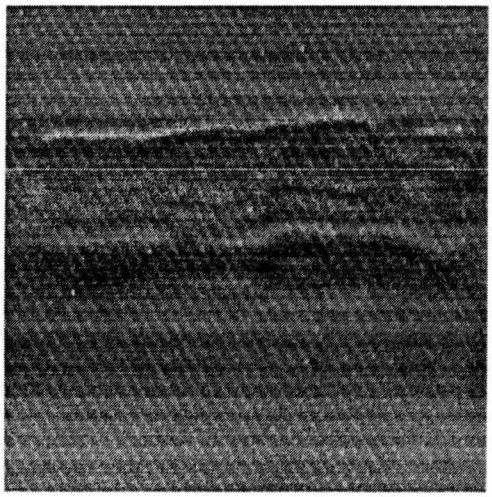
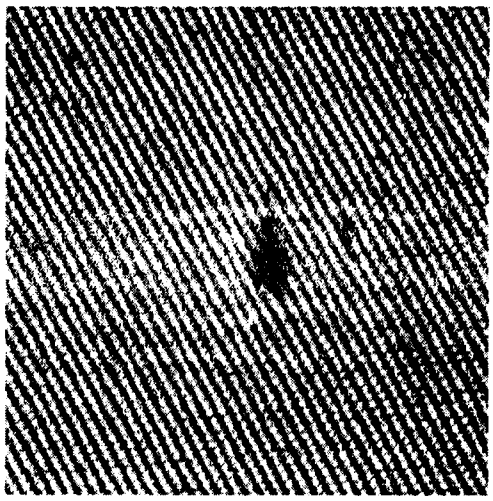


Figure 3.9: An image of a fabric with a knot and its histogram



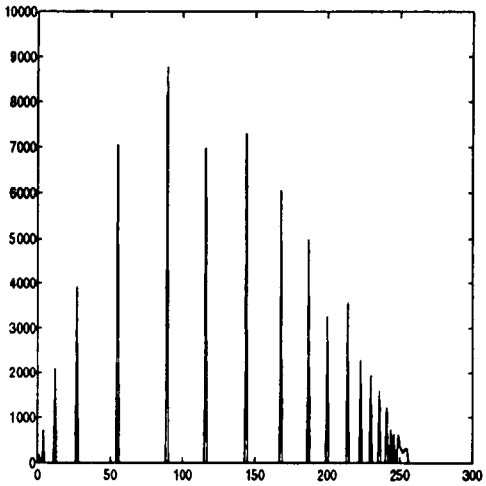


Figure 3.10: The image after histogram equalization and its histogram

3.2 Thresholding

An important step in image analysis is segmentation, which is aimed at separating the picture into two areas, the threads and the pores between them. The simplest approach to segmenting an image is the use of gray-level thresholding, which is a process that compares the gray level of a pixel with a given value (threshold) and labels the pixel 'white' if its gray level is above the threshold and 'black' otherwise. A simple threshold image $G_{i,j}$ is defined as

$$G_{i,j} = \begin{cases} 1 & \text{if } X_{i,j} > T \\ 0 & \text{if } X_{i,j} <= T \end{cases}$$

the i and j are coordinates, $X_{i,j}$ is original gray level of pixel (i, j), and T is threshold.

The selection of the threshold value is usually made from the histogram. The simplest of all thresholding techniques is to partition the image by using a single threshold, T. There are a number of methods to select an optimal threshold [11]. In this project, in order to preserve the size and shape of defects, the selection of the threshold should guarantee that almost all the pixels in the defective area in the image are categorized as 'black'. Therefore, the threshold is determined by the gray level distribution of pixels in defective area. In the training stage, the user will extract defective areas from sample images and calculate the mean and standard deviation of the pixels in these areas.

As illustrated in Figure 3.11, the threshold was set by

$$T = \mu + z * \sigma$$

where μ and σ are the mean and standard deviation of gray levels of pixels in the defective areas, respectively.

The factor z is chosen according to the gray level ditribution of pixels in the defetive areas. Table 3.1 shows the statistics of the gray level distribution of pixels in the defective areas. With the choice of the factor 2.17, only 2.0% of the pixels in the defective area will have gray level higher than T, and 98.0% of the pixels in defective area will be categorized as 'black' ones. After thresholding, the shape and size of defects on the fabric will not be reduced.

Sometimes it is difficult to extract defective areas from the sample images during the training stage. Careful examination of the defective pixel gray

level distribution suggests that a defective pixel usually has gray level less than the average of the maximum and minimum gray levels of the image. This means it is fairly safe to choose the mean-gray-level as the threshold to categorize all pixels in the defective area as 'black'.

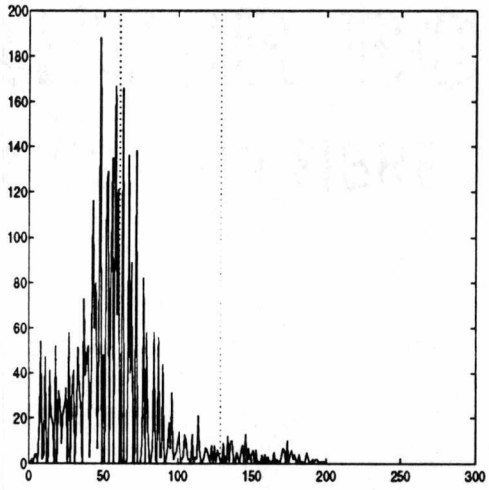


Figure 3.11: Gray level distribution of pixels in defective areas

Table 3.1: The comparison of distribution of pixels in defective areas with the normal distribution

Range	Distribution of Pixels in Defective Areas
$< \mu + \sigma$	0.8764
$< \mu + 2\sigma$	0.9732
$< \mu + 3\sigma$	0.9890
$< \mu + 4\sigma$	0.9978

Figures 3.12, 3.13 and 3.14 show an example of thresholding. Figure 3.12 shows a simple fabric image, and Figure 3.13 shows its histogram. The range of gray levels is [0, 255]. Figure 3.14 shows the result of segmenting Figure 3.12 by using a threshold $T = 129$, which achieved a 'clean' segmentation by eliminating the shadows between threads. The selection of this threshold is illustrated in Figure 3.11.

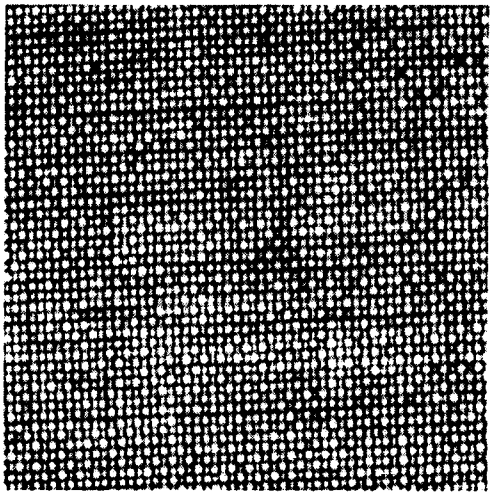


Figure 3.12: Histogram equalized image

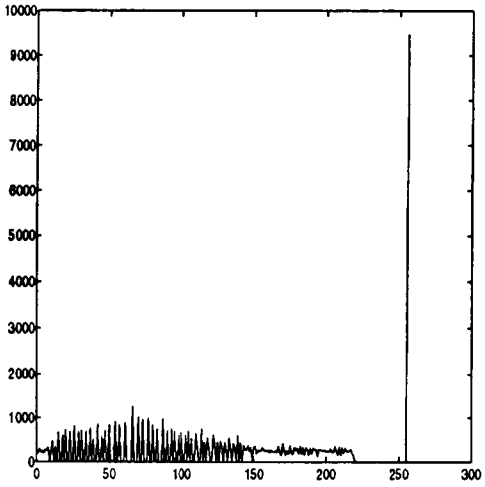


Figure 3.13: Gray level histogram of equalized image

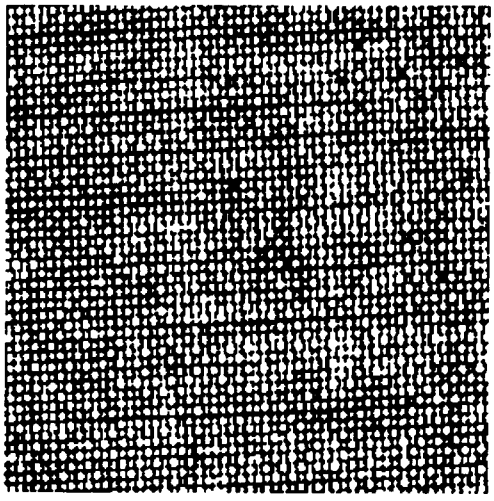


Figure 3.14: Result of histogram equalization and segmentation with T=129

3.3 Morphology

From a general scientific perspective, the word 'morphology' refers to the study of form and structure. The same word in the context of mathematical morphology means a tool for extracting image components that are useful in the representation and description of region shape [11]. Basic morphological operations include dilation, erosion, opening and closing. The morphological operations can be employed for many purposes, including edge detection, segmentation, enhancement and noise removal in images. The morphological operations used in this project are erosion and opening.

3.3.1 Erosion and Dilation

Erosion and dilation are the bases for most of the morphological operations, including opening and closing. Erosion is an operation to erode a binary image by a structuring element and dilation is one to dilate a binary image by a structuring element [9].

Let Z^2 denote the set of all ordered pairs of elements (a, b), with a and b being integers from the set of real integers Z.

Suppose the object A and the structuring element B are represented as sets in Z^2. Let $(B)_x$ denote the translation of B so that its origin is located at x. Let $\hat{B}$ denote the reflection of B so that $\hat{B} = \{x | x = -b,\ b \in B\}$. The erosion of A by B, denoted as $A \ominus B$, is defined as the set of all points x such that $(B)_x$ is included in A, that is:

$$A \ominus B = \{x | (B)_x \subseteq A\}.$$

The dilation of the image A by the structuring element B, denoted as $A \oplus B$, is defined as the set of all points x such that $(\hat{B})_x$ and A have nonempty intersection:

$$A \oplus B = \{x | (\hat{B})_x \cap A \neq \phi\}.$$

Figures 3.15 and 3.17 show an example of erosion. Figure 3.15 is a equalized and thresholded image, which is then subjected to erosion by a structuring element of size 6X6 shown in Figure 3.16. Figure 3.17 shows the eroded image. Since the structuring element is bigger than the dark elements in the background of the image, only the thick slub in the center of the image remains in the result image. The slub was eroded down to a thinner one.

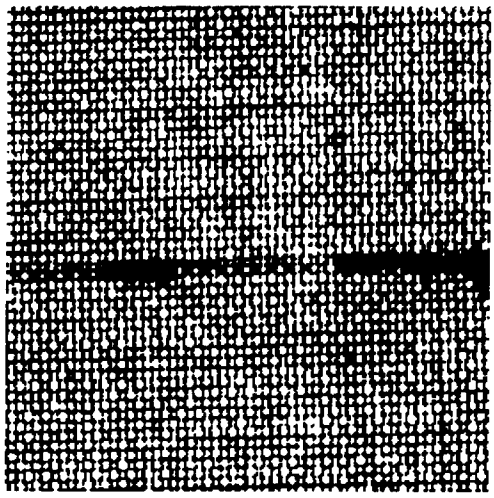


Figure 3.15: A equalized and thresholded image



Figure 3.16: Structuring element of size of 6X6

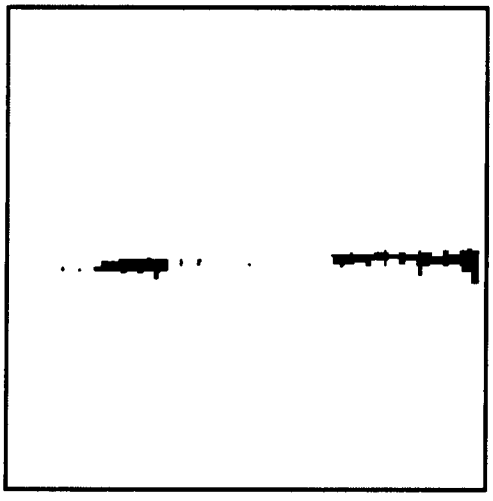


Figure 3.17: Image subjected to erosion by structuring element of size 6X6

3.3.2 Opening and Closing

In addition to the two fundamental operations of erosion and dilation, two other important operations are opening and closing, which are defined by the combination of erosion and dilation.

The opening of set A by structuring element B, denoted by $A \circ B$, is defined as erosion of A by B, followed by a dilation of the result by B:

$$A \circ B = (A \ominus B) \oplus B.$$

The closing of set A by structuring element B, denoted by $A \bullet B$, is defined as dilation of A by B, followed by the erosion of the result by B:

$$A \bullet B = (A \oplus B) \ominus B.$$

Figure 3.18 shows the result of opening of Figure 3.15 by a structuring element of size 6X6. The image is first eroded by the structuring element and then the result of erosion is dilated by the structuring element. The thiner slub in the result of erosion is dilated to a similar thickness of the slub in the original image. By carefully choosing the structuring element, we can eliminate the background and keep the subject in the image.

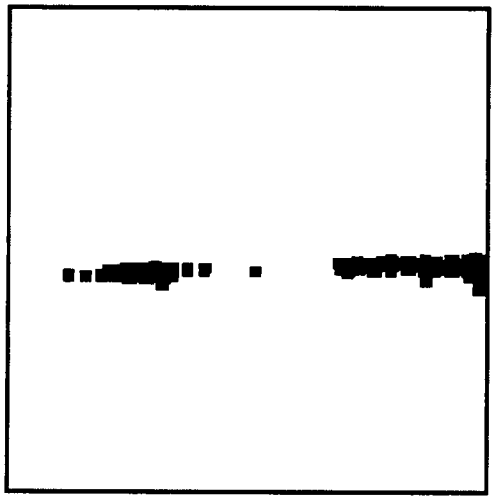


Figure 3.18: Image subjected to opening by structuring element of size 6X6

3.4 Autocorrelation

Texture may be defined with respect to the global properties of an image or to the repeating units that compose it. Fabric texture is a recurring spatial pattern. It is necessary to determine the repeat lengths of patterns. Andrews [1] presented a method to determine the repeat lengths in a periodic construction by evaluating a two-dimensional co-occurrence matrix. In this project, autocorrelation function is employed to determine the horizontal and vertical repeat lengths in fabric images.

The autocorrelation function of an image is defined as

$$C_{k,l} = \sum_i \sum_j X_{i,j} X_{i-k,j-l}$$

where $X_{i,j}$ is the gray level value of pixel(i,j) in image.

Let $C_{x,0}$ and $C_{0,y}$ denote the autocorrelation function in horizontal and vertical directions. $C_{x,0}$ and $C_{0,y}$ are defined as:

$$C_{x,0} = \sum_i \sum_j X_{i,j} X_{i-x,j}$$

and

$$C_{0,y} = \sum_i \sum_j X_{i,j} X_{i,j-y}$$

Since woven fabric consists of two systems of yarns, warps and fillings, the repeat unit has the same orientation as that of the fabric. Therefore, the behaviors of autocorrelation functions in vertical and horizontal directions are studied to determine the size of the repeat unit in the fabric image. Figure 3.19 illustrates a plain weave pattern. If this pattern is perfectly repeated in the fabric image, which means each repeat unit in the image has exactly same gray level, $C_{x,0}$ will have maximum value when $x = km$, where k=0, 1, 2,..., and $C_{0,y}$ will reach maximum value when $y = kn$, where k=0, 1, 2,.... Therefore, we can determine the repeat unit size by observing the interval between peaks in $C_{x,0}$ and $C_{0,y}$.

Figure 3.20 shows an example of a fabric image. Figure 3.21 and 3.22 show the Autocorrelation function $C_{x,0}$ and $C_{0,y}$ of the sample image. $C_{x,0}$ and $C_{0,y}$ have maximum value when x and y are 0, which shows that gray level of pixels in the image always have highest correlation with itself. In Figure 3.21, the second peak appears at x=9 and third at x=18. There is

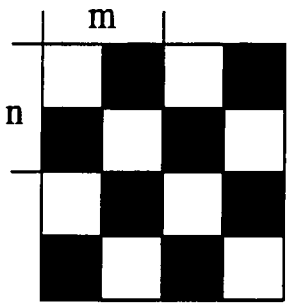


Figure 3.19: An example of a repeat pattern

a local peak at x=4. Since it is lower than peaks on its both sides, it is considered as a local peak. We see that the height of the peaks decline when x increases. This suggests that the repeat unit is not perfectly repeated in the image and gray level of pixels are less correlated to their remote counterparts because of increasing chance of mismatch. The rate of the decline of associated peaks reveals the degree of regularity in the image. In Figure 3.22, the second peak appears at y=11 and the third at y=22, and the magnitudes of the alternative peaks decrease faster than that in Figure 3.21, which shows that the regularity in horizontal direction is better than that in vertical direction. By observing the interval between peaks in Figure 3.21 and 3.22, we conclude that this fabric image has repeat unit of size 11X9.

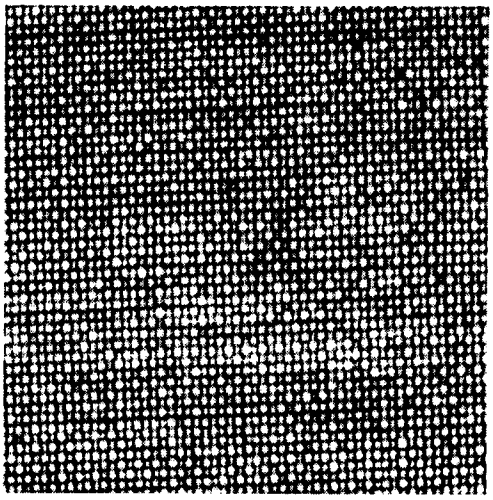


Figure 3.20: An example of fabric image

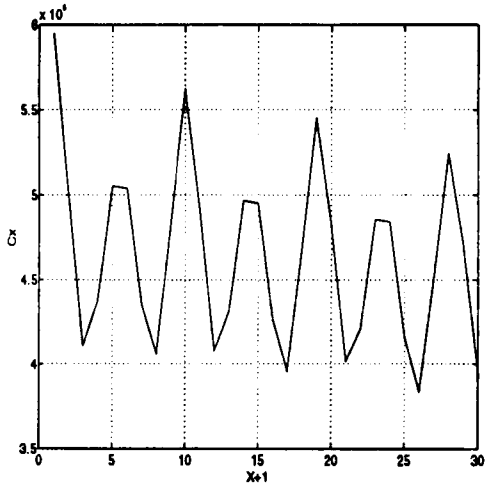


Figure 3.21: Autocorrelation function $C_{x,0}$ of sample image

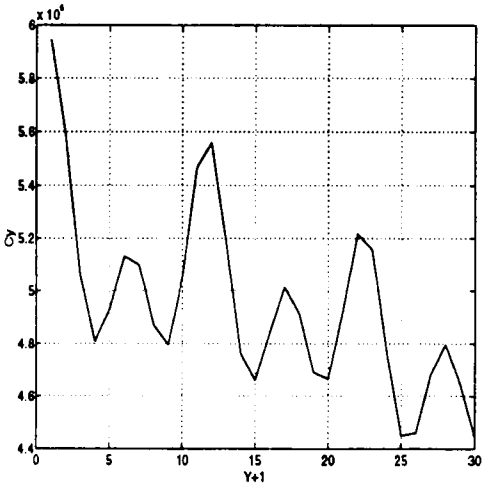


Figure 3.22: Autocorrelation function $C_{0,y}$ of sample image

CHAPTER 4

Instrumentation and Experiment Design

4.1 Instrumentation

A typical image-processing system contains three fundamental elements: an image-acquisition element, an image-processing element and an image-display element. A picture is converted to a digital image and stored in a memory by the image-acquisition element. This image is displayed in some form by the image-display element for human viewing. The image-processing element is designed to carry out image analysis tasks.

4.1.1 Hardware

The image-processing system used in this project consists of a Sun SPARC2 Unix Workstation produced by Sun Microsystems Co., a MTI Series 68 video camera from Dage-MTI Inc. in Michigan City, Indiana, a Fujinon-TV Zoom Lens system from Fuji Photo Optical Co., a 90100 EX-C6 extension tube set from Asahi Precision Co., Ltd., a Ikegami model PM-127 monitor from Ikegami Tsushinki Co., Ltd., a PCvision Plus frame grabber and a IBM386 PC to store the image temporarily. The MTI Series 68 Video Camera has a 1100 line resolution. The frame grabber provides a total storage of 512 X 480 pixels with eight bits (equivalent to 256 gray levels) for each pixel. The frame grabber digitizes the incoming video signal at a rate of 30 frames per second. The image of a sample taken by the video camera through the zoom lens system is sent to PCvision interface and digitized by the A/D converter within it. The digitized image is stored in the frame grabber and displayed on monitor. The image is then transferred to Sun SPARC2 Unix Workstation for image processing.

In the process of image-acquisition, the sample illumination affects the image brightness and contrast. The samples are illuminated with transmitted light by using Beseler PS360 Projector (Charles Beseler Co., Florham Park, New Jersey). Five pieces of rough-surface glass sheets are placed above the light bulb to generate uniform light by scattering. A voltage converter is used to control the illumination level and the voltage powering the

illumination system is checked and adjusted regularly.

4.1.2 Software

This project uses the Khoros Visual Programming System and Software Development Environment for Data Processing and Visualization Release 1.0 developed by University of New Mexico in 1991. Software for calculating autocorrelation function and making gray level statistical testing have been developed by the author. Matlab from Mathwork, Inc., Natick, MA. is used to process and plot test results.

4.2 Experimental Material

4.2.1 Material

All the test samples are from Cherokee Textile Mill in Sevior County, Tennessee. Two sets of fabric are tested: plain weave and twill weave.

4.2.2 Detecting Fabric Defects

Two approaches have been studied. The first approach is a gray level statistical approach; and second one is a morphological operation approach.

As illustrated in Figure 4.1, the original image is first histogram equalized. The first approach has two stages: training stage and testing stage.
1. Training Stage. In this stage, autocorrelation functions $C_{x,0}$ and $C_{0,y}$, as defined in section 3.4 are calculated to determine the size of repeat unit. Overlap windows of the same size of the repeat unit are arranged as illustrated in Figure 4.2. Overlap windows are used to avoid missing the defects lying on the edge of neighboring windows.

If repeat unit is perfectly repeated in the fabric image, the mean of gray level of pixels in each window should be the same. Due to variation of illuminating level and image noise, the gray level mean in each window lies within a parallelpiped area. By testing nondefective fabric samples, we can obtain the expected gray level mean in each window and its standard deviation. The upper limit and lower limit of the parallelpipe can be set as $\mu + z\sigma$ and $\mu - z\sigma$. The selection of value z depends on the strictness of defect detecting test.

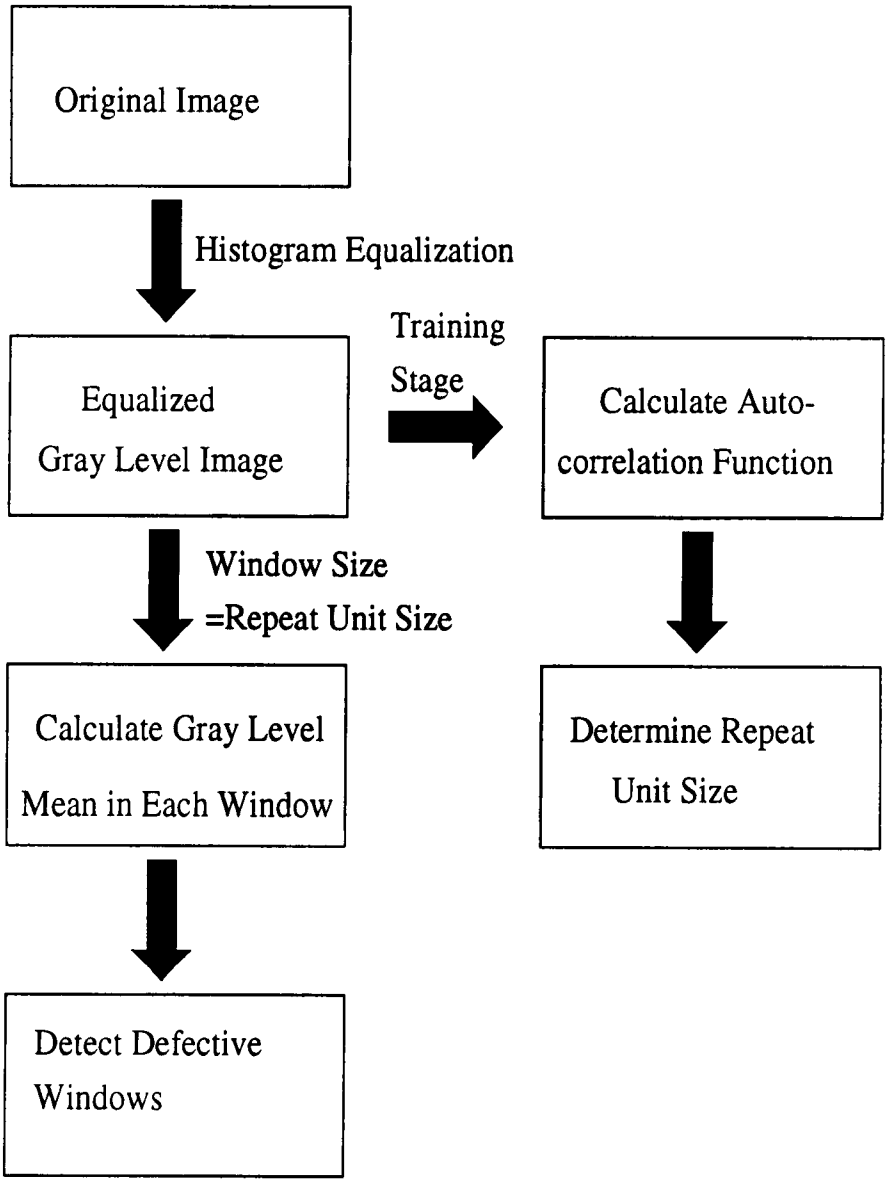


Figure 4.1: Gray level statistical approach

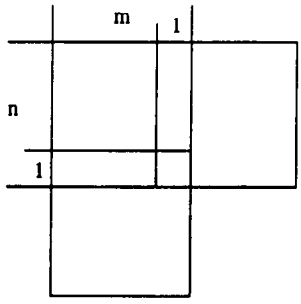


Figure 4.2: Illustration of overlap windows

2. Test Stage. In this stage, the image is also divided into segments as illustrated in Figure 4.2. In each of these overlap windows, one calculates the gray level mean and checks whether the value lies between upper and lower limit of parallelpipe obtained in the learning stage. If this is the case, then the segment does not have defects. Otherwise, this segment will be marked defective.

Figure 4.3 illustrates the morphological operation approach. In this approach, the image goes through the histogram equalization first. Then gray level thresholding maps the gray scale image into a binary image. The selection of threshold has been discussed in section 3.2. Erosion is applied to the binary image to eliminate dark pixels in the background. If the eroded image has more than a certain number of dark pixels remaining in it and if these dark pixels concentrate in a small region, then this image will be categorized as defective. Dilation can be applied to the eroded image to obtain the original shape and size of the defects.

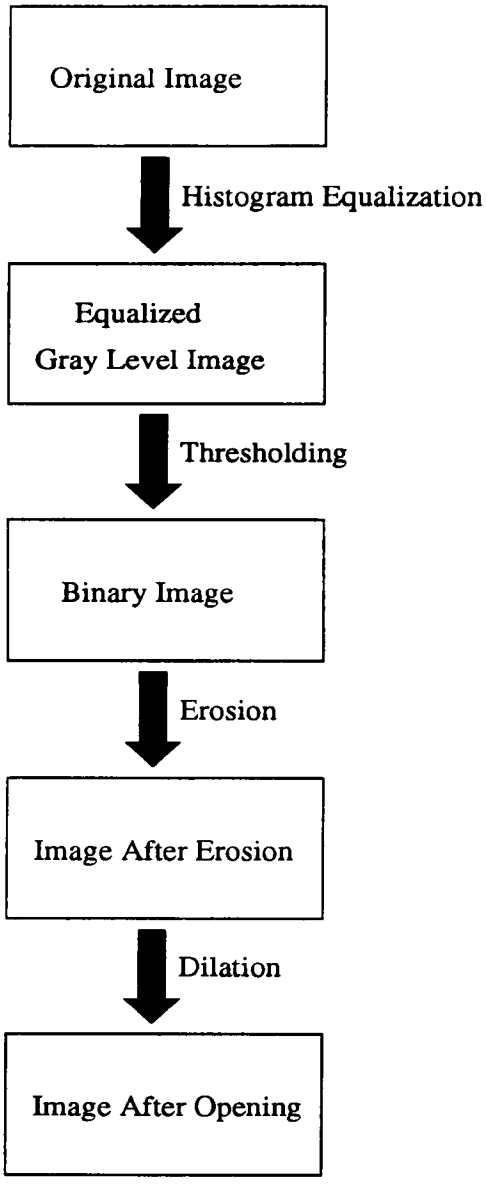


Figure 4.3: Morphological operation approach

CHAPTER 5

Results and Discussion

5.1 Gray level statistical approach

5.1.1 Repeat unit size and selection of test window size

The method to determine the repeat unit size has been described in section 3.4. The overlap test windows are arranged as illustrated in section 4.2.2. The test windows are set to the same size of the repeat unit. If a fabric image has perfect periodic construction, which means each repeat unit in the image has exactly same set of gray levels, each test window will have the same average gray level. Due to the variation of illumination level and image noise, repeat unit is not perfectly repeated in the image and the average gray level in each test window will lie in a parallelpiped area.

The width of the parallelpiped area depends on the standard deviation of the average gray level in each window. If standard deviation is low, which means the fabric image has higher regularity, all average gray levels in test windows lie between a narrow parallelpiped area. A narrow parallelpiped area makes it possible to detect defective windows which are slightly deviant from the normal pattern. In general, when the size of the test window increases, the standard deviation of average gray level in each window will decrease. However, a test window should not be too large. It will be difficult to detect small defects by using large test windows, since the defective pixels will be a smaller portion in the window and have smaller impact to the average gray level. It is also difficult to detect the shape of defects by using large test windows.

Repeat unit size is the perfect size for the test windows. The fabric samples in this project are solid-shade and unpatterned textiles. The repeat unit sizes of these fabrics only depend on their weave pattern and they will not be too large. The standard deviation of average gray level in each repeat unit is low, since each repeat unit has pixels of similar gray levels to those in other units. Table 5.1 summarizes the standard deviations of the average gray level in windows of different sizes. The fabric sample used here is plain weave sample A, which has repeat unit size of 11X9. We see that

when window size increases, the standard deviation of average gray level decreases. However, using window size 11X9 makes the standard deviation (13.56) smaller than those of window sizes 11X10 (14.19) and 12X9 (13.60).

Table 5.1: The standard deviations of gray level average in windows of different size.

Window Size	σ	Window Size	σ	Window Size	σ
11X2	42.65	2X9	31.95		
11X4	17.63	4X9	19.68		
11X6	18.50	6X9	16.02		
11X8	15.37	8X9	16.30	9X9	15.12
11X9	13.56	10X9	14.05	10X10	14.75
11X10	14.19	11X9	13.56	11X11	14.75
11X12	13.73	12X9	13.60		
11X14	12.77	14X9	13.45		

5.1.2 Lower limit of the average gray level in the test window

Careful examination of the defective pixel gray level distribution suggests that a defective pixel usually has a gray level less than a normal pixel. Therefore, only the lower limit of the average gray level in the test window is needed to detect the deviant windows. The lower limit of the parallelpiped area can be set as $\mu - z\sigma$. The selection of factor z depends on the strictness of the test. If the factor z is small, the lower limit of the average gray level will be high. It will be sensitive enough to detect slightly deviant windows and reveal the shape of the defects. In the meantime, it will also cause more false alarms. If the factor z is large, the lower limit of the average gray level will be low. It will have fewer false alarms because it is more tolerant to slightly deviant windows. However, it will misclassify some defective windows as normal because of its wider acceptance range.

Table 5.2 summarizes the test results of using a different lower limit. Nine specimens from plain weave sample A are tested, using factor z of different values: 3.60, 3.54 and 3.10. Assume the distribution of average gray level in windows is normal distribution. With the choice of these z factors, 99.99%, 99.98% and 99.90% of the normal windows will be categorized as defect-free and only 0.01%, 0.02% and 0.1% normal windows will be misclassified.

Table 5.2: Test results using different lower limits.

Samples	*Category*	$\mu - 3.60\sigma$		$\mu - 3.54\sigma$		$\mu - 3.10\sigma$	
		DD	MC	DD	MC	DD	MC
A1	Slub	14	0	15	0	17	0
A2	Slub	4	0	6	0	12	3
A3	Slub	7	0	8	0	11	2
A4	Knot	5	1	5	2	5	3
A5	Normal	0	0	0	0	0	1
A6	Normal	0	0	0	0	0	1
A7	Normal	0	0	0	0	0	1
A8	Normal	0	0	0	0	0	2
A9	Normal	0	0	0	0	0	1
Total		30	1	34	2	45	11

DD: Number of defective windows detected.
MC: Number of test windows misclassified.

The mean(μ) and standard deviation(σ) of sample A are listed in Table 5.3. From the results shown in Table 5.2, we see that by using factor z of 3.54, more defective windows are detected than using factor z of 3.60 and fewer normal windows are misclassified than using factor z of 3.10.

Figure 5.1 shows an image of a fabric with a slub. Figures 5.2, 5.3 and 5.4 show the test results of using different lower limit of the average gray level in windows. In Figure 5.2, four defective windows are detected and there are no false alarm. In Figure 5.3, six defective windows are detected, which reveals more details about the shape and size of the defect. In Figure 5.4, more windows are categorized as defective, and three of them are misclassified normal windows.

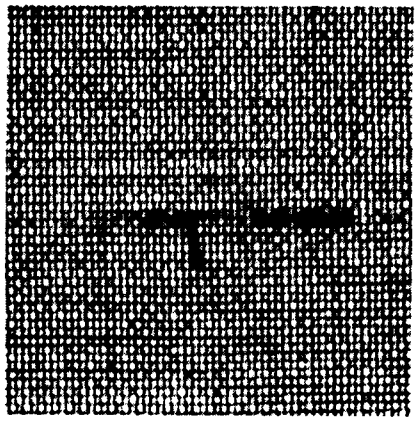


Figure 5.1: A simple image of a fabric with a slub

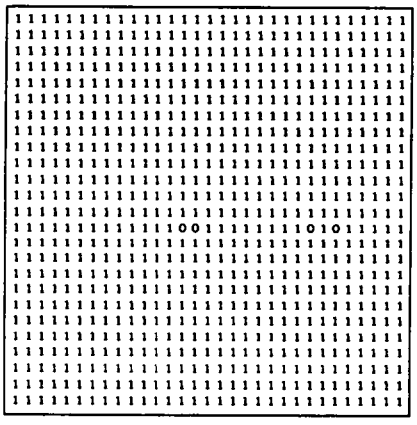


Figure 5.2: Test result of using factor z of 3.60

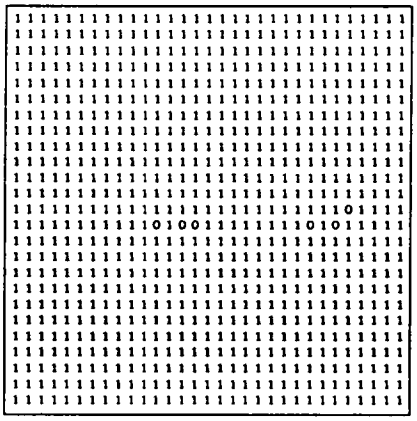


Figure 5.3: Test result of using factor z of 3.54

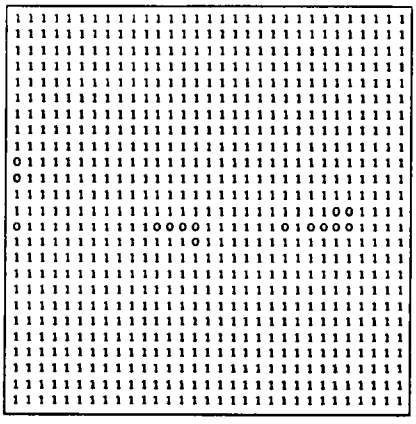


Figure 5.4: Test result of using factor z of 3.10

5.1.3 The connectivity between defective windows and defects classification

After the defective windows are detected and indicated, defective windows which belong to the same defect need to be grouped together to test the size and shape of the defect. The D_4 distance, or city-block distance is employed to measure the distance between test windows. Let p and q, with coordinates (x, y) and (s, t), denote two test windows in the sample image. The D_4 distance between p and q is defined as

$$D_4(p, q) = |x - s| + |y - t|.$$

Fabrics are formed by two systems of yarns in vertical and horizontal directions. The defects that we study here, knots and slubs, are more likely to occur along the same direction of the yarns. The D_4 distance is employed because the defective windows on the same horizontal or vertical axes are more likely to be from the same defect than those on the same diagonal axis.

Defective window p merges into one defective window groups, if

(1) there exists a defective window q in that group and

(2) the D_4 distance between p and q is less than or equal to 3.

A defective window, which has no neighbor defective windows with D_4 distance ≤ 3, is considered a false alarm and ignored. The length of the defect is determined by the distance between the leftmost and rightmost defective windows in the group and the width of the defect by the distance between the upmost and lowest defective windows.

If the length of the defect is more than two times the width of the defect, or the width is more than two times the length, the defect is categorized as slub. Otherwise, it is a knot. If one slub is detected, all the other defective window groups on the same axis can merge with this slub and only one slub is indicated.

Figure 5.5 shows an image of a fabric with a slub and Figure 5.6 shows the distribution of average gray levels in the test windows. The gray level statistical test result is shown in Figure 5.7. The defective windows in the image will merge into two groups. The size of the defect on the left side of the image is 5X2 and the one on the right side has size of 9X1. Both of them are categorized as slubs. Since they are on the same axis, they can merge together and have the new size of 25X2. Only one slub will be indicated.

Figures 5.8, 5.9 and 5.10 show another example of test result. Figure 5.10 shows the gray level test result. The defective windows in the middle

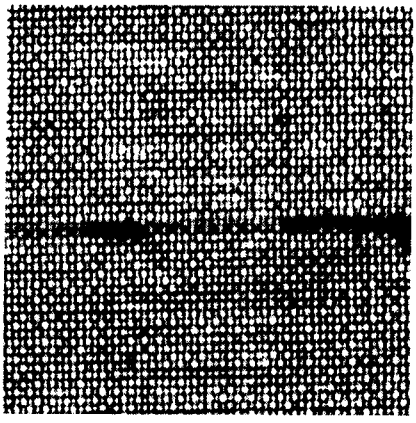


Figure 5.5: An example of a fabric with a slub

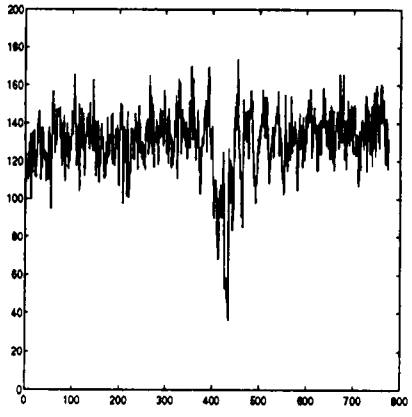


Figure 5.6: Average gray level in each window

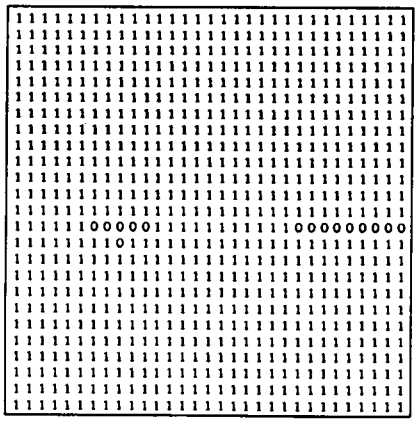


Figure 5.7: Gray level statistical test result

of the image merge into one group with size of 3X2. It is categorized as knot. The single defective window at the right side of the image has no neighboring defective windows with D_4 distance ≤ 3 and it is ignored.

Figures 5.11 - 5.16 show more test results of the twill weave samples.

Table 5.3: The repeat unit size and statistics of samples

	Samples	Repeat Unit Size	μ	σ	$\mu - 3.54\sigma$
Plain Weave	A	11X9	131.0	13.56	84.36
	B	16X12	130.13	19.57	60.80
	C	8X5	130.28	19.43	61.50
	D	7X5	128.60	33.76	9.10
	E	8X7	129.59	22.00	51.71
Twill Weave	F	14X7	137.14	14.18	86.94
	G	15X6	130.41	17.80	67.40
	H	19X11	133.92	25.17	44.82
	I	15X6	129.47	24.38	43.16

More experiments have been done to two sets of samples: plain weave and twill weave. Eight specimen of each sample are tested. The repeat unit size and statistics of samples are listed in Table 5.3. The test results are listed in Table 5.4. From the test results, we can see that the gray level statistical detecting approach has a high detection rate and a low false alarm rate.

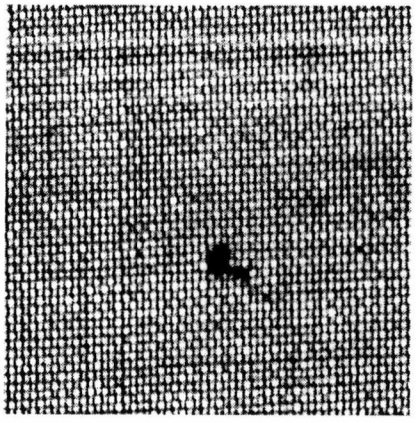


Figure 5.8: An example of a fabric with a knot

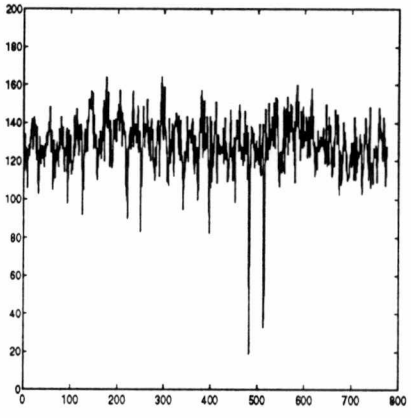


Figure 5.9: Average gray level in each window

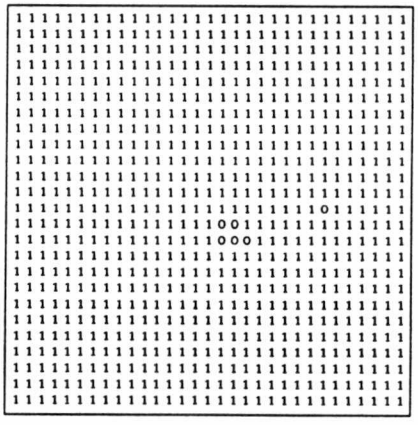


Figure 5.10: Gray level statistical test result

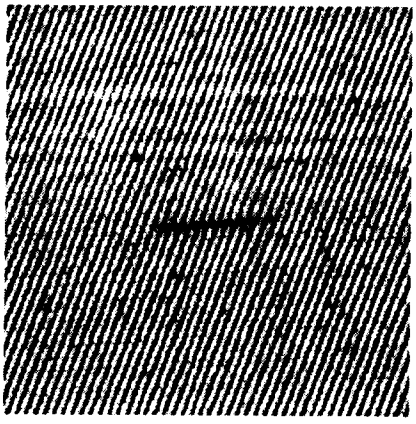


Figure 5.11: An example of a fabric with a slub

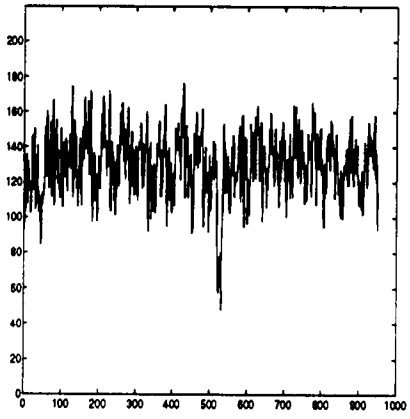


Figure 5.12: Average gray level in each window

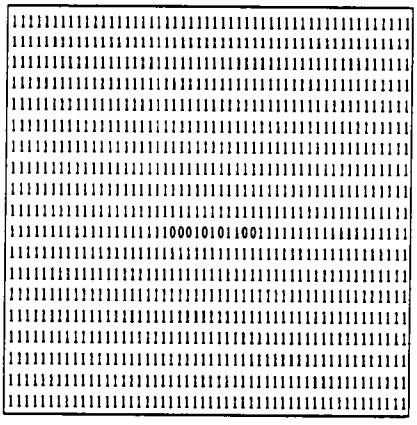


Figure 5.13: Gray level statistical test result

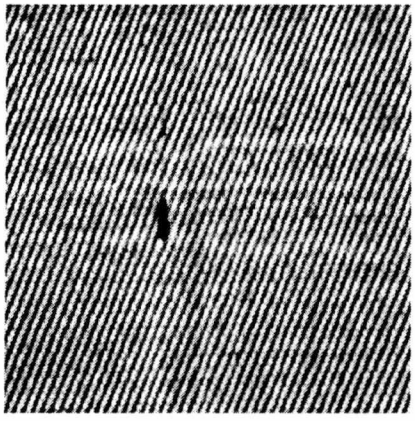


Figure 5.14: An example of a fabric with a knot

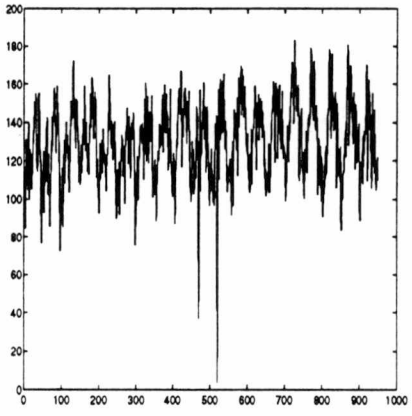


Figure 5.15: Average gray level in each window

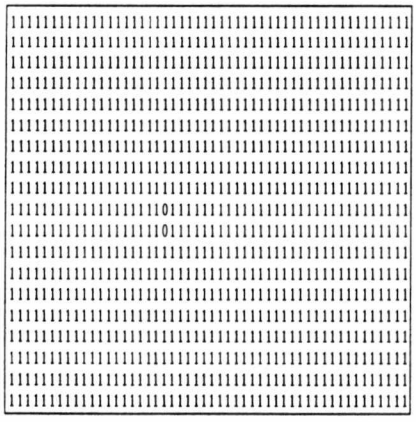


Figure 5.16: Gray level statistical test result

Table 5.4: The gray level statistical test results

	Samples	Defective Samples		Test Results		Normal Samples	False Alarm
		Slub	Knot	Slub	Knot		
Plain Weave	A	3	1	3	1	5	0
	B	1	1	1	1	6	0
	C	2	0	2	0	6	0
	D	1	3	1	3	4	0
	E	2	2	2	1	4	0
Twill Weave	F	2	2	2	2	4	0
	G	3	1	3	1	4	0
	H	0	4	0	3	4	1
	I	1	1	1	1	6	0
Total		15	15	15	13	43	1

5.2 Morphological operation approach

All the images are histogram equalized and mapped into a binary image by gray level thresholding. The selection of the threshold has been discussed in section 3.2. Erosion is applied to these binary images to eliminate the background dark pixels. Dilation can be applied to eroded images to obtain the size and shape of the defects.

5.2.1 The selection of kernel size

The key step of this approach is to select the size and shape of the kernel, or structuring element. Fabrics are formed by interlacing horizontal and vertical yarn systems. After thresholding, yarns in the fabric and their shadow form a dark background in the fabric image. The defects create bigger spots of dark areas in the image than normal fabrics. A kernel of the rectangular shape should be set to the right size, big enough to erode the background dark spots and small enough to keep the defects in the eroded image.

An autocorrelation function can be employed here to determine the size of the dark spots in the background. As described in section 3.4, gray levels of pixels in the image always have highest correlation with itself and lowest correlation with the pixels of the opposite value. Therefore, the distance between the peak and the bottom of curve in the autocorrelation function reveals the size of the dark strings in the background of the image. Figures 5.17 and 5.18 show the autocorrelation function of a twill weave sample G, listed in section 5.2.2. The slopes of the peak declining in these two functions are small, which means the sample has high regularity in both horizontal and vertical directions. In Figure 5.17, the first peak appears at x=0 and the second at x=6, and the first bottom of curve appears at x=3 and the second at x=9. It suggests that the vertical black strings in the background of the image have a thickness of 3 pixels. Figure 5.18 shows the autocorrelation function $C_{0,y}$ of sample G. The distance between the peak and the bottom of the curve is 8, which suggests that the black horizontal strings in the background have a thickness of 8 pixels. To guarantee that all the black strings in the background of the image will be eliminated, the kernel for this image should have a minimum size of 8X3.

Figures 5.19, 5.20, 5.21 and 5.22 show the images subjected to opening by a kernel of different sizes. The minimum kernel size is 8X3. We see that the black strings can not be totally eliminated if the smaller kernel is used.

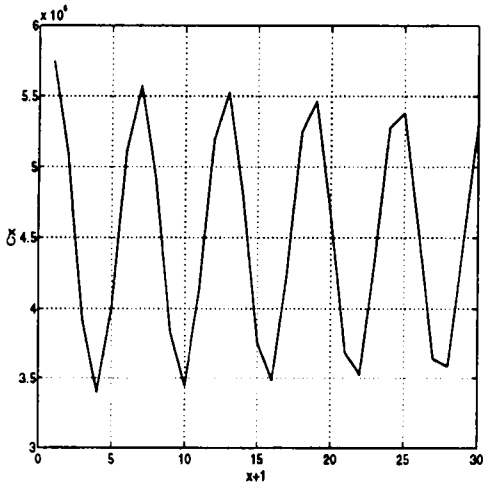


Figure 5.17: Autocorrelation function $C_{x,0}$ of twill weave sample G

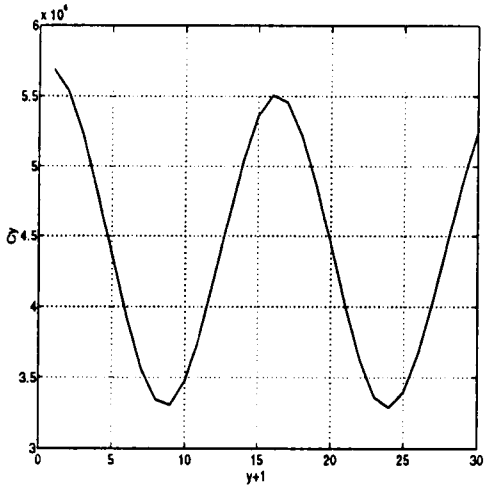


Figure 5.18: Autocorrelation function $C_{0,y}$ of twill weave sample G



Figure 5.19: An image of a fabric with a slub

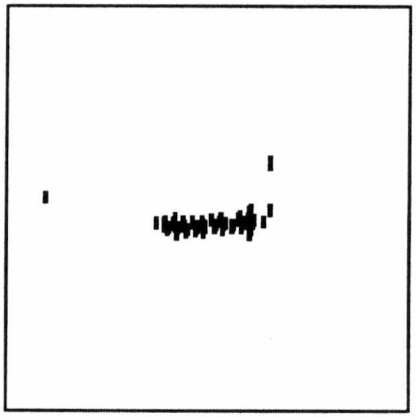


Figure 5.20: Image subjected to opening by structuring element of 8X3

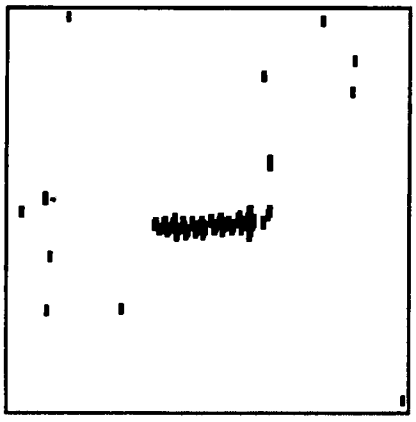


Figure 5.21: Image subjected to opening by structuring element of 7X3

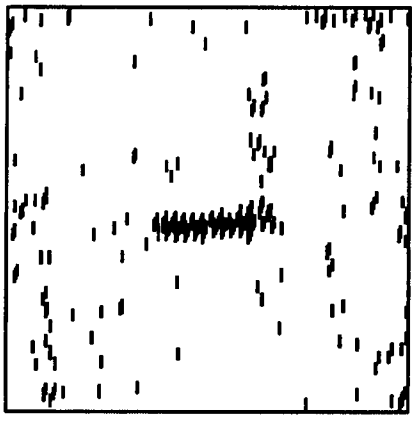


Figure 5.22: Image subjected to opening by structuring element of 8X2

5.2.2 Detection and classification of defects

Two sets of samples, plain weave and twill weave are subjected to the experiment. The repeat unit size, minimum kernel size and test kernel size are listed in Table 5.5.

Table 5.5: The repeat unit size and kernel size of samples

	Samples	Repeat Unit Size	Minimum Kernel Size	Test Kernel Size
plain Weave	A	11X9	3X2	6X6
	B	16X12	6X2	7X3
	C	8X5	4X3	5X4
	D	7X5	4X3	5X4
	E	8X7	4X2	5X4
Twill Weave	F	14X7	7X4	8X5
	G	15X6	8X3	8X4
	H	19X11	9X7	9X8
	I	15X6	8X3	8X4

After the images are subjected to erosion, most black strings in the background are eliminated. A dilation is then applied to the eroded image. The remaining dark pixels in the image subjected to opening should be grouped to test the size and shape of the defect. The D_4 distance is employed to measure the distance between pixels. Dark pixel p merges into one group if

(1) there exists a dark pixel q in that group and

(2) the D_4 distance between p and q is less and equal to d.

Factor d can be chosen by the users according to the quality of the images and the strictness of the test. In this case, factor d is set as 8. If a dark pixel group has less than n times the kernel size, the group will be ignored. The selection of factor n depends on the strictness of the test. In this case, factor n is set as 4. The length of the defect is determined by the distance between the leftmost and the rightmost dark pixels in the group and the width by the distance between the upmost and the lowest pixels in the group.

If the length of the defect is more than two times the width of the defect, or the width is more than two times the length, the defect is categorized as a slub. Otherwise, it is a knot. If one slub is detected, all the other defects on the same axis can merge with this slub and only one slub is indicated.

Figures 5.23, 5.24 and 5.25 show an image of a fabric with a slub and images subjected to erosion and opening. The kernel size is set as 8X4, slightly larger than the minimum kernel size. After erosion, all dark strings in the background are eliminated and only the subject remains in the image. All the dark pixels in the image can merge into one group, since all of them have one another dark pixel within the D_4 distance of 8. The size of this dark pixel group is 521 pixels, which is more than four times greater the kernel size (4x8x4=128). The length of the defect is 60 pixels and the width is 18 pixels. The length/width ratio is greater than 2. This defect is categorized as a slub.

An image of a fabric with a knot is shown in Figure 5.26. Images subjected to erosion and opening are shown in Figures 5.27 and 5.28. All darked pixels in the image subjected to opening can group together. The size of the dark pixel group is 244 pixels, more than four times greater the kernel size. The length of the defect is 14 pixels and the width is 26 pixels. This defect is categorized as a knot.

Figures 5.29 – 5.31 show an example of morphological operation on a plain weave sample with a slub. In Figure 5.31, the remaining dark pixels in the image subjected to opening can merge into five groups. Two dark pixel groups in the middle of the image have size greater than four times of kernel size. The left group is categorized as knot and the right one is categorized as slub. Since the knot is on the same axis as the slub, they can merge into one slub. The other three dark pixel groups are ignored because they have sizes smaller than four times that of the kernel size. Another example is shown in Figure 5.32 – 5.34.

More tests have been done and the test results are listed in Table 5.6. From the test results, we see that the morphological approach has a high defects detection rate. Some false alarms happened to three samples. All images of these three samples have a high noise level. After thresholding, many noise pixels are categorized as dark pixels. Some of these noise are big enough to remain in the image after opening and be misclassified as defects.

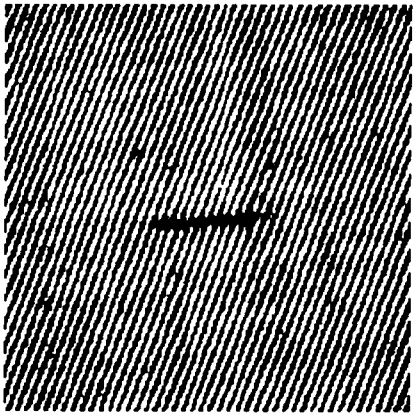


Figure 5.23: An example of a fabric with a slub

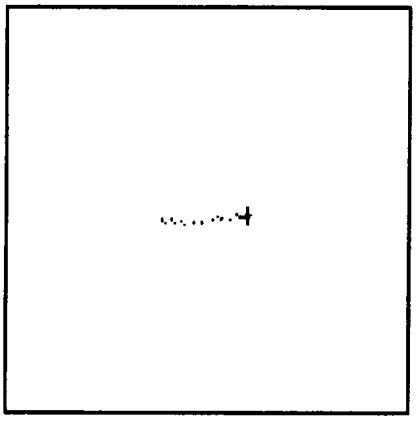


Figure 5.24: Image subjected to erosion by structuring element of size 8X4

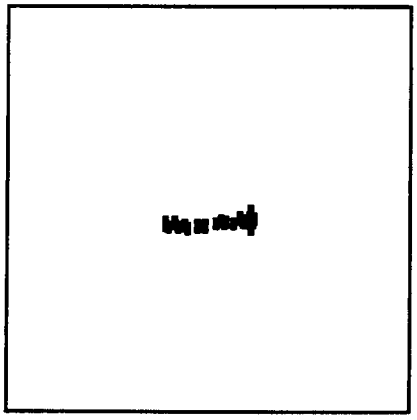


Figure 5.25: Image subjected to opening by structuring element of size 8X4

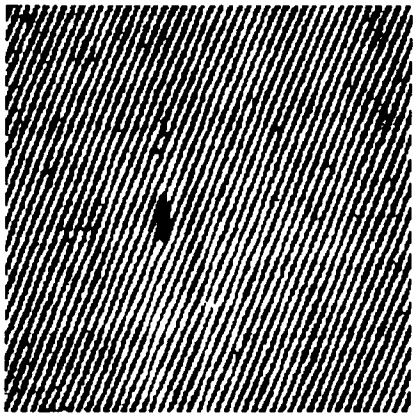


Figure 5.26: An example of a fabric with a knot

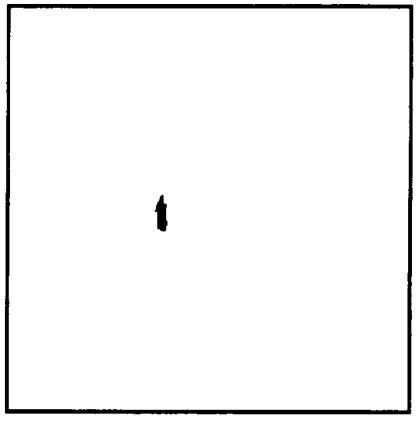


Figure 5.27: Image subjected to erosion by structuring element of size 8X4

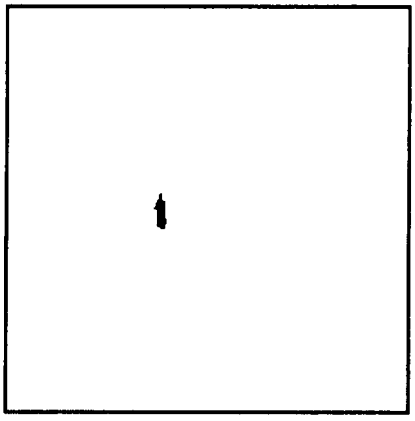


Figure 5.28: Image subjected to opening by structuring element of size 8X4

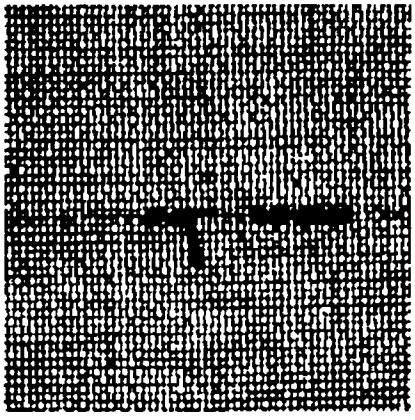


Figure 5.29: An example of a fabric with a slub

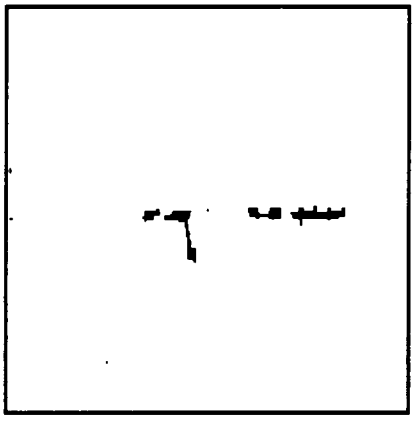


Figure 5.30: Image subjected to erosion by structuring element of size 6X6

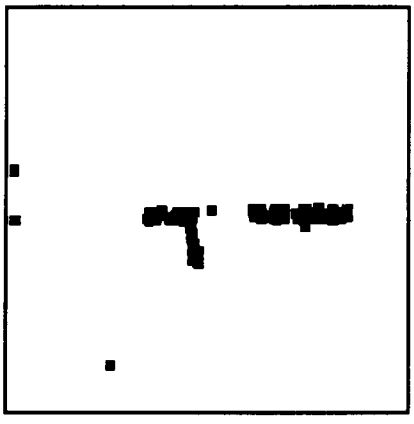


Figure 5.31: Image subjected to opening by structuring element of size 6X6

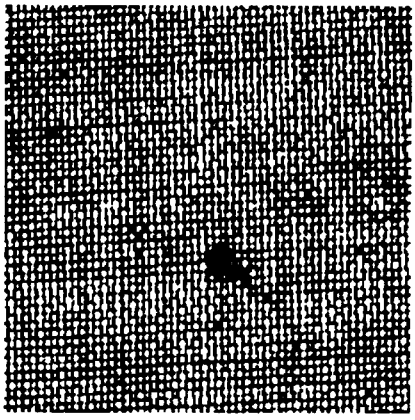


Figure 5.32: An example of a fabric with a knot

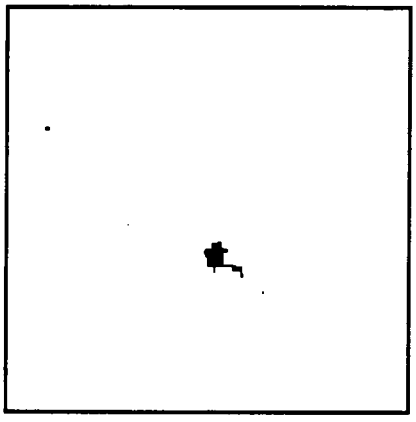


Figure 5.33: Image subjected to erosion by structuring element of size 6X6

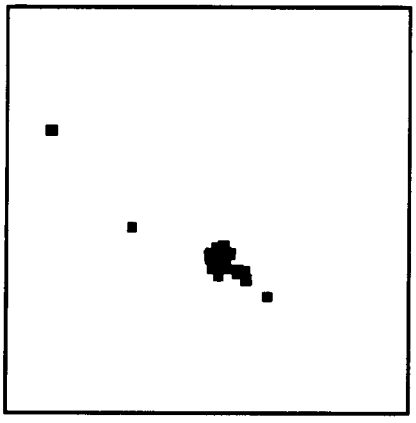


Figure 5.34: Image subjected to opening by structuring element of size 6X6

Table 5.6: The morphological operation test results

	Samples	Defective Samples		Test Results		Normal Samples	False Alarm
		Slub	Knot	Slub	Knot		
Plain Weave	A	3	1	3	1	5	0
	B	1	1	1	1	6	0
	C	2	0	2	0	6	0
	D	1	3	1	3	4	3
	E	2	2	2	1	4	2
Twill Weave	F	2	2	2	2	4	0
	G	3	1	3	1	4	0
	H	0	4	0	4	4	1
	I	1	1	1	1	6	0
Total		15	15	15	14	43	6

CHAPTER 6

Summary and Recommendations

6.1 Summary

Two defect detecting approaches have been presented and discussed. Two sets of fabric samples, plain weave and twill weave are tested. An autocorrelation function is employed to determine the repeat unit size in the fabric images. In the gray level statistical approach, the overlay windows are of the same size as the repeat unit size. It is illustrated by some experiments that repeat unit size is a proper size for test windows. The lower limit of the average gray level in the windows can be set according to the strictness of the test. If the lower limit is too high, it will create many false alarms. If the lower limit is too low, it will not be sensitive enough to detect small defects. In this project, test results of using different lower limit are compared and $\mu - 3.54\sigma$ seems to achieve the best performance. After the defective windows are detected, they are grouped together to test the size and shape of the defects. A defective window is accepted or rejected from a group, according to the shortest D_4 distance between this defective window and the windows in that group. The gray level statistical approach has shown that it is sensitive to the defects and tolerant of the noise. It has a high detection rate and a low false alarm rate.

The key step in the morphological approach is to select a structuring element or kernel of the right size. An autocorrelation function is used to determine the width of the black strings in the background of the image after thresholding. The minimum kernel size is set for each sample according to size of the black strings. Experiments using kernels of different sizes have shown that the test kernel size should be one or more pixels larger in both dimensions than the minimum kernel size. The morphological approach is also sensitive to defects. In comparison with the gray level statistical approach, the morphological approach requires more uniform fabric images with low noise level. Image noise and shadow can be misclassified as defects and will cause false alarms. In comparison with the gray level statistical approach, the morphological approach takes more time in training stage

and it is also slower in the defects detecting process.

This study has shown that image analysis is able to provide a reliable, objective way to detect fabric defects. Many experiments have been carried out to show the good separability between defects and normal fabrics.

6.2 Recommendations

The task is particularly suitable for parallel processing as the image can be divided up into equal parts and each can be analyzed in the same way.

Although the tests in the project are limited to plain weave and twill weave unpatterned and solid-shade fabric samples, the system has the potential to detect defects in small patterned fabrics. More experiments of using samples of different weave patterns are suggested. The defects studied in this project are mainly knots and slubs. The system may also be able to detect other defects by the same approach. More experiments using samples with different defect types are recommended.

BIBLIOGRAPHY

BIBLIOGRAPHY

[1] Andrews, Lutz, "Contribution Concerning the Detection of Defects on Small-patterned textiles". *Milliand Textile*, Vol. 72, pp. 981-984, 1991.

[2] "Standard Terminology Relating to fabric Defects". *ASTM*, Vol. 07.02, pp. 217-223, 1991.

[3] Blackmon, A. G., *Manual of Standard Fabric Defects in the Textile Indudtry*, Graniteville Company, Graniteville, South Carolina, 1975.

[4] Cheng, Luo and Randall Bresee, "Appearance Evaluation by Digital Image Analysis". *Textile Chemist and Colorist*, Vol. 22, No. 2, pp. 17-19, 1990.

[5] Chin, Roland T. and Charles A. Harlow, "Automated Visual Inspection: A Survey". *IEEE Transaction on Pattern Analysis and Machine Intelligence*, Vol. PAMI-4, No. 6, pp. 557-573, 1982.

[6] Conners, Richard W. and Charles W. McMillin, Kingyao Lin, "Identifying and Locating Surface Defects in Wood: Part of an Automated Lumber Processing System". *IEEE Transaction on Pattern Analysis and Machine Intelligence*, Vol. PAMI-5, No. 6, pp. 573-583, 1983.

[7] Don, Hon-Son and King-Sun Fu, C. R. Liu, Wei-Chung Lin, "Metal Surface Inspection Using Image Processing Techniques". *IEEE Transactions on Systems, Man, and Cybernetics*, Vol. SMC-14, No. 1, pp. 139-146, 1984.

[8] Editors of American Fabrics Magazine, *Encyclopedia of Textiles.* Prentice-Hall, Inc., Englewood Cliffs, New Jersey, 1970.

[9] Giardina, C. R. and E. R. Dougherty, *Morphological Methods in IMage and Signal Processing.* Prentice Hall, Englewood Cliffs, New Jersey.

[10] Gong, R. H. and A. Newton, "Image-analysis Techniques Part I: The Measurement of Pore-size Distribution". *Journal of Textile Institute*, Vol. 83, No. 2, pp. 253-268, 1992.

[11] Gonzalez, Rafael C. and Richard E. Woods, *Digital Image Processing.* Addison-Wesley Publishing Company, Reading, Massachusetts, 1992.

[12] Haralick, R. M. and K. Shanmugam, "Textural Features for Image Classification". *IEEE Trans. Syst. Man, Cybernet*, Vol. 3, pp. 610-621, 1973.

[13] Pavilidis, T., *Algorithm for Graphics and Image Processing.* Computer Science Press, Rockville, MD, 1982.

[14] Harlock, S. C. and D. N. Gisbourne, "An Image-analysis Technique Applied to the Measurement of the Pile-fibre Distribution in Silver-knitted Fabric". *Journal of Textile Institute*, Vol. 80, No. 4, pp 585-593, 1989.

[15] Hinze, Dieter, "Objective Assessment of the Warp Stripiness of Woven Fabrics by Means of Digital Image Processing". *Melliand Textile*, Vol. 73, pp. 33-36, 1992.

[16] Hinze, Dieter and Heidrum Mehlhorn, Steffen Burkhardt, "Digital Image Processing by Means of a Parallel Computer System for the Testing of Fabrics", *Milliand Textile*, Vol. 72, p. 993, 1991.

[17] Huang, Xuan-chao and Randall R. Bresee, "Characterization Nonwoven Web Structure Using Image Analysis Techniques". *INDA Journal*, Vol. 5, No. 3, pp. 28-38, 1993.

[18] Jarvis, J. F., "A Method for Automating the Visual Inspection of Printed Wiring Boards". *IEEE Trans. Pattern Anal. Machine Intell.*, Vol. PAMI-2, pp. 77-82, 1980.

[19] Kaasjager, Anton, "Textile Fabric Monitoring with Image Analysis" *Milliand Textile*, Vol. 71, pp. 64-66, 1990.

[20] McVey, E. S., "An Experimental Printed Circuit Board Drilling System Automated by pattern recognition". *Pattern Recognition*, Vol. 11, pp 271-276, 1979.

[21] Okawa, Toshikuni, "Automatic Inspection of the Surface Defects of Cast Metals". *Computer Vision, Graphics, and Image Processing*, Vol. 25, pp. 89-112, 1984.

[22] Robson, D. and P. J. Weedall, R. J. Harwood, "Cuticular Scale Measurements Using Image Analysis Techniques". *Textile Research Journal*, pp. 713-717, 1989.

[23] Rosler, Ulrich, "Defect Detection of Fabrics by Image Processing". *Melliand Textile*, Vol. 73, p. 635, 1992.

[24] Sterling, W. M., "Automatic Non-reference Inspection of Printed Wiring Boards". *Proc. IEEE Comput. Soc. Conf. Pattern Recognition and Image Processing*, August, pp. 93-100, 1979.

[25] Schicktanz, Karlheinz, "Practical Experience with Automatic Cloth Inspection by the Laser-scan System." *Melliand Textile*, Vol. 71, pp. 786-789, 1990.

[26] Sobus, J. and B. Pourdeyhimi, J. Gerde, Y. Ulcay, "Assessing Changes in Texture Periodicity Due to Appearance Loss in Crapet: Gray Level Co-occurence Analysis". *Textile Research Journal*, October, pp. 557-567, 1991.

[27] Taylor, R. A., "Estimating the Size of Cotten Trash with Video Images". *Textile Research Journal*, April, pp. 185-193, 1991.

[28] Taylor, Robert A. and Luther Godbey, "Video Scan Trashmeter Area Calibration". *Textile Research Journal*, November, pp. 646-653, 1990.

[29] Tobin, Kenneth W., "How Oak Ridge National Lab Fosters Automated Inspection". *Advanced Imaging*, July, pp. 48-51 1993.

[30] Watanabe, Akira and Shi-Nya Kurosaki, Fujio Konda, "Analysis of Blend Irregularity in Yarns Using Image Processing. Part I: Fundamental Investigation of Model Yarns". *Textile Research Journal*, Vol. 62, pp. 690-696, 1992.

[31] Watkins, L. S., "Inspection of IC Photomasks with Intensity Spatial Filters". *Proc. IEEE*, Vol. 57, pp. 1634-1639, 1969.

[32] West, R. N. and W. J. Stocker, "Automatic Inspection of Cylinder Bores". *Metrol Inspection*, July, 1977.

[33] Wiese, David R., "Automating The Inspection Of Carpets-With Lasers". *America's Textile International*, March, pp. 82-85, 1988.

[34] Wood, Errol J., "Applying Fourier and Associated Transforms to Pattern Characterization in Textiles". *Textile Research Journal*, April, pp. 212-220, 1990.

[35] Wood, Errol J. and Robert M. Hodgson, "Carpet Texture Measurement Using Image Analysis". *Textile Research Journal*, January, pp. 1-11, 1989.

[36] Wu, Y. and B. Pourdeyhimi, S. M. Spivak, "Texture Evaluation of Carpets Using Image Analysis". *Textile Research Journal*, Vol. 61, No. 7, pp. 407-419, 1991.

VITA

Yixiang Frank Zhang was born in Shanghai, China, on February 20, 1966, to Mr. and Mrs. Yuqi Zhang as their second son. He graduated from the Affiliated High School of Shanghai Normal University, Shanghai, in 1984. He attended China Textile University, Shanghai from 1984 to 1988 and received a Bachelor of Science degree in Textile Material Science as an honor graduate. He worked in Shengzhen, Guangdong, China from 1988 to 1989. In January, 1990 he entered the Graduate School at the Univisity of Tennessee, Knoxville and he was awarded a Teaching Assistantship. In October, 1990 he was awarded a Research Assistantship from the Consortium Project of Melt Blown and Spunbond Nonwovens from the Recycled Polymers. He received a Master's degree in Textile Science in December, 1991. He entered the Department of Computer Science in the University of Tennessee in January, 1992 and he was awarded a Teaching Assistantship. In December 1993 he received a Master's degree in Computer Science.